Science of the Total Environment xxx (xxxx) xxx

Contents lists available at ScienceDirect

Science of the Total Environment

journal homepage: www.elsevier.com/locate/scitotenv

Impact of an extreme monsoon on CO_2 and CH_4 fluxes from mangrove soils of the Ayeyarwady Delta, Myanmar

Clint Cameron [a,*], Lindsay B. Hutley [a], Niels C. Munksgaard [a], Sang Phan [b], Toe Aung [c], Thinn Thinn [c], Win Maung Aye [c], Catherine E. Lovelock [b]

[a] Research Institute for the Environment and Livelihoods, Charles Darwin University, Darwin, Northern Territory, Australia
[b] School of Biological Sciences, The University of Queensland, St Lucia, QLD 4067, Australia
[c] Watershed Management Division, Forest Department, Ministry of Natural Resources and Environmental Conservation, Nay Pyi Taw, Myanmar

HIGHLIGHTS

- We measured GHG fluxes from soils of mature, converted and rehabilitating mangroves in Myanmar.
- Assessments were conducted during the dry (February) and wet season (October).
- High soil CO_2 emissions in February from an 8 year old site were likely due to substantial belowground carbon allocation.
- All sites had high rates of soil CO_2 efflux in October due to freshwater influx and alluvium deposition.
- Methane emissions increased significantly during an extreme wet season.

GRAPHICAL ABSTRACT

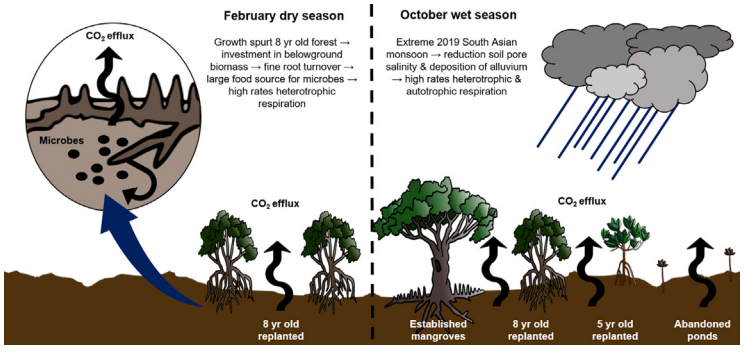

ARTICLE INFO

Article history:
Received 19 August 2020
Received in revised form 21 October 2020
Accepted 23 October 2020
Available online xxxx

Editor: Manuel Esteban Lucas-Borja

Keywords:
Mangroves
Myanmar
Greenhouse gas emissions
Monsoon
Seasonal variation

ABSTRACT

Mangrove ecosystems can be both significant sources and sinks of greenhouse gases (GHGs). Understanding variability in flux and the key factors controlling emissions in these ecosystems are therefore important in the context of accounting for GHG emissions. The current study is the first to quantify GHG emissions using static chamber measurements from soils in disused aquaculture ponds, planted mangroves, and mature mangroves from the Ayeyarwady Delta, Myanmar. Soil properties, biomass and estimated net primary productivity were also assessed. Field assessments were conducted at the same sites during the middle of the dry season in February and end of the wet season in October 2019. Rates of soil CO_2 efflux were among the highest yet recorded from mangrove ecosystems, with CO_2 efflux from the 8 year old site reaching 86.8 ± 17 Mg CO_2 ha^{-1} yr^{-1} during February, an average of 862% more than all other sites assessed during this period. In October, all sites had significant rates of soil CO_2 efflux, with rates ranging from 31.9 ± 4.4 Mg CO_2 ha^{-1} yr^{-1} in a disused pond to 118.9 ± 24.3 Mg CO_2 ha^{-1} yr^{-1} in the 8 year old site. High soil CO_2 efflux from the 8 year old site in February is most likely attributable to high rates of primary production and belowground carbon allocation. Elevated CO_2 efflux from all sites during October was likely associated with the extreme 2019 South Asian monsoon season which lowered soil pore salinity and deposited new alluvium, stimulating both autotrophic and heterotrophic activity. Methane efflux increased significantly (50–400%) during the wet season from all sites with mangrove cover, although was a small overall component of soil GHG effluxes during both measurement periods. Our results highlight the critical importance of assessing GHG flux in-situ in order to quantify variability in carbon dynamics over time.

* Corresponding author.
E-mail address: clint.cameron@cdu.edu.au (C. Cameron).

https://doi.org/10.1016/j.scitotenv.2020.143422
0048-9697/

1. Introduction

Mangroves can be both significant sources and sinks of greenhouse gases (GHGs) (Mukhopadhyay et al., 2002), with the exchange of GHGs between soil, water and the atmosphere a function of the complex interplay between autotrophic production and allocation, respiration from mangrove roots (pneumatophores and below ground fine root aerenchyma) and heterotrophic respiration from microbial, macrofaunal and fungal activity. The magnitude and direction of GHG flux varies over multiple spatial and temporal scales (Bulmer et al., 2017) and is driven by a number of biogeochemical variables which interact at local (e.g. soil water content, salinity gradients, fine root production, microbial and macrofaunal communities), regional (e.g. geomorphology, precipitation, tidal inundation), and latitudinal scales (e.g. temperature, Spivak et al., 2019, Ochoa-Gomez et al. 2019). Additionally, anthropogenic land use change (e.g. conversion of mangroves to aquaculture ponds) is widely recognised as the most significant proximate driver of GHG emissions in mangrove ecosystems (Kauffman et al., 2014; Sidik and Lovelock, 2013). Disturbance to soils fundamentally alters the state and interactions between biogeochemical factors, resulting in large emissions of carbon to the atmosphere (Cameron et al., 2019a).

Land use change and resultant GHG emissions is particularly important for countries such as Myanmar which has among the highest rate of mangrove conversion of any nation in the world, with an annual rate of loss estimated at 0.75% (Goldberg et al., 2020; Hamilton and Casey, 2016). Mangrove loss in Myanmar has primarily been through conversion to rice agriculture (Richards and Friess, 2016), with approximately 98% of deforestation due to agricultural field expansion and the remaining 2% to aquaculture (Webb et al., 2014). Mangrove conversion has largely been concentrated within the fertile alluvium soils of the Ayeyarwady River Delta (Estoque et al., 2018), one of the largest deltaic systems in South East Asia. Mangroves thrive in deltaic environments with high allochthonous sediment inputs (Alongi, 2009), and the Ayeyarwady Delta once supported 274,781 ha of mangrove forest which extended upstream by up to 60 km (Zöckler and Aung, 2019). However, conversion of mangroves in the delta between 1980 and 2013 resulted in the loss of 229,733 ha, or over 83% of original extent (Webb et al., 2014). Tropical cyclone Nargis (2008), the most destructive natural disaster in the recorded history of Myanmar, also caused an estimated 35,000 ha of mangrove loss across the country in addition to high losses of human live (Zöckler and Aung, 2019). Extraction for timber, charcoal production, fishing pole construction, and residential settlements are also identified as key drivers of ongoing mangrove loss (Zöckler and Aung, 2019). Resultant emissions from mangrove conversion for the country between 2000 and 2012 are estimated at 35.6 Mt CO_2e (Friess et al., 2020), equivalent to 24.2% of total reported carbon emissions (147.1 Mt CO_2e) over the same period for Myanmar (Ritchie and Roser, 2017).

While the conservation of intact mangroves and rehabilitation of degraded areas is gaining prominence as a means to offset national GHG emissions, empirically quantifying GHG dynamics in mangrove ecosystems under differing land uses and assessment of the influence of biophysical variables – particularly seasonality - remains limited to a handful of studies (Sasmito et al., 2019). This study addresses such knowledge gaps through quantifying, comparing and contrasting GHG fluxes across gradients of biophysical variables, land uses, and seasons in the Ayeyarwady Delta of Myanmar, a country where no previous studies have been conducted. We aimed to assess the influence of key biophysical variables on GHG flux, specifically soil characteristics (carbon, nitrogen, and bulk density) and mangrove biomass accumulation, across a range of land use treatments and at differing times of the year. Assessments were conducted during the middle of the dry season in February, and the end of the wet season in October 2019. We predicted that rehabilitating mangroves would exhibit the highest rates of CO_2 efflux given (a) developing forests exhibit higher productivity and rates of soil respiration than established forests (Pregitzer and Euskirchen, 2004), and (b) the addition of autochthonous respiration increases total soil respiration, as opposed to purely heterotrophic respiration observed in disused ponds with no mangrove cover.

2. Materials and methods

2.1. Site context

The current study was located in the Ayeyarwady River Delta (Fig. 1). The Ayeyarwady River extends across the entire length of Myanmar and is the country's most important commercial waterway (Sirisena et al., 2018). The drainage basin encompasses 410,000 km^2, 91% of which is located in Myanmar, and at its confluence with the Andaman Sea forms one of the most extensive deltaic systems in Southeast Asia (Sirisena et al., 2018). The lower Ayeyarwady River basin has a humid tropical climate, with temperatures ranging from a mean of 25 °C in January to 30 °C in April (Owen et al., 2019). Average annual precipitation between 2009 and 2017 at Pyapon, the closest city to the study location where rainfall records area available, was 533 mm (World Weather Online, 2020). Seasonal precipitation is dominated by the South Asia summer monsoon which results in peak rainfall falling between May and October. High seasonal rainfall elevates water levels in the Ayeyarwady River from mid-June to mid-October upwards of 6 to 9 m above the lowest water levels which occur in February (Owen et al., 2019). These monsoonal freshwater pulses carry significant alluvial sediment loads which overflow river banks on high tides, depositing allochthonous sediment and resulting in the rapid accretion and seaward expansion of the delta into the Andaman Sea at rates upwards of 50 m per year (Owen et al., 2019).

2.2. Climatic conditions during the study period

The 2018 monsoon season resulted in over 300 mm more rainfall than average (total 857.2 mm) at Pyapon (Fig. 2), while in 2019 monsoonal rainfall was 2231 mm which is three times the average rainfall for the area between 2009 and 2017 (World Weather Online, 2020). The extreme 2019 monsoon resulted in extensive flooding across much of Myanmar and displaced an estimated 231, 202 people (IFRC, 2019). Our measurements conducted in October 2019 were thus influenced by this extreme monsoon event.

2.3. Study location and sampling design

We surveyed soils and vegetation in natural and regenerating mangroves as well as aquaculture ponds in 89 randomly selected plots in the area of three townships (Bogale, Pyapon and Labuta) in the lower Ayeyarwady Delta (Fig. 1). For assessment of GHG fluxes, we focused on a site in close proximity to a Department of Forestry field station that had been replanted with mangroves under the 'Integrated Mangrove Rehabilitation and Management Project through Community Participation in the Ayeyarwady Delta Project 2013–2017' (APFNet, 2017). Three distinct land-use treatments from 5 sites were assessed. With reference to Table 1 and Fig. 1, these were: former aquaculture ponds that were replanted with mangroves 5 (a) and 8 (b) years before the time of sampling; a mature stand of riverine mangroves (c); and two disused aquaculture ponds (d and e) under different inundation regimes.

2.4. Community structure, above and below ground mangrove biomass, and estimates of net primary productivity

At the 5 and 8 year old rehabilitating sites, assessments of mangrove forest composition and above and below ground biomass were conducted following methods developed by Kauffman and Donato (2012). Replicate plots of 5 m radius were established in which species and diameter at breast height (DBH, measured at 1.3 m above the

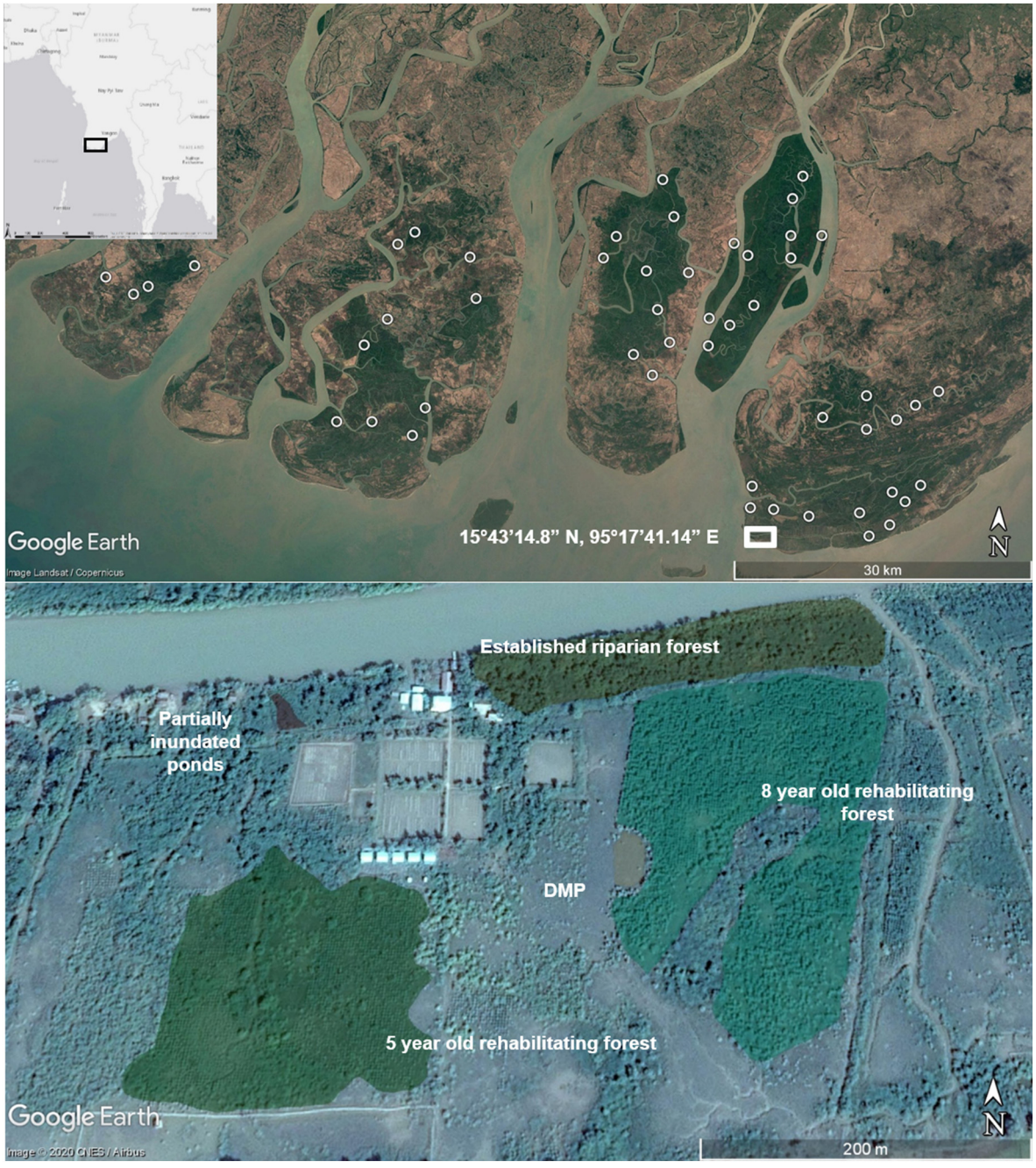

Fig. 1. Location of soil and vegetation sampling plots (white circles) within the Ayeyarwady Delta, Myanmar, and study site for greenhouse gas fluxes (white box in top image, and lower image).

ground) for all trees were measured. Nested sub-plots with a 2 m radius were established at the centre of each plot to record seedling and sapling density. Allometric equations were used to calculate above and below biomass using both species specific equations and common (mangrove generic) equations (Komiyama et al., 2005). The carbon content of biomass was calculated by multiplying by a factor of 0.464 for aboveground biomass and 0.39 for belowground biomass (Kauffman and Donato, 2012). Carbon stock change in biomass over an 8- and 5-year period following restoration from aquaculture ponds respectively was used as a basis to estimate Net Primary Production (NPP). A multiplier of 32.3% was used to estimate leaf litter production, the key missing component of NPP from our measurements of rehabilitating mangroves, based on the global average allocation of NPP to leaf litter in mangrove forests (Alongi, 2014) *in lieu* of site-specific field measurements. Biomass accumulation for established mangroves was estimated for stands between 16 and 30 years old from a restoration chronosequence (GGKP, 2020).

2.5. Greenhouse gas flux measurements

Soil GHG flux measurements were conducted at the same sites during two field trips in February and October 2019. For the February campaign, an INNOVA 1412i photoacoustic infra-red gas analyser (LumaSense Technologies, Inc., CA, USA) was used, while a Li-Cor 7810 Trace Gas Analyser (Li-Cor, Inc., Nebraska, USA) was used for assessments in October. The INNOVA measured the concentration of three gases (CO_2, N_2O, and CH_4,) and water vapour (H_2O), while the Li-Cor measured CO_2, CH_4 and H_2O. The INNOVA was calibrated for each gas species prior to use in the field using Zero Air (blank) and two certified standards of different concentrations in either air or

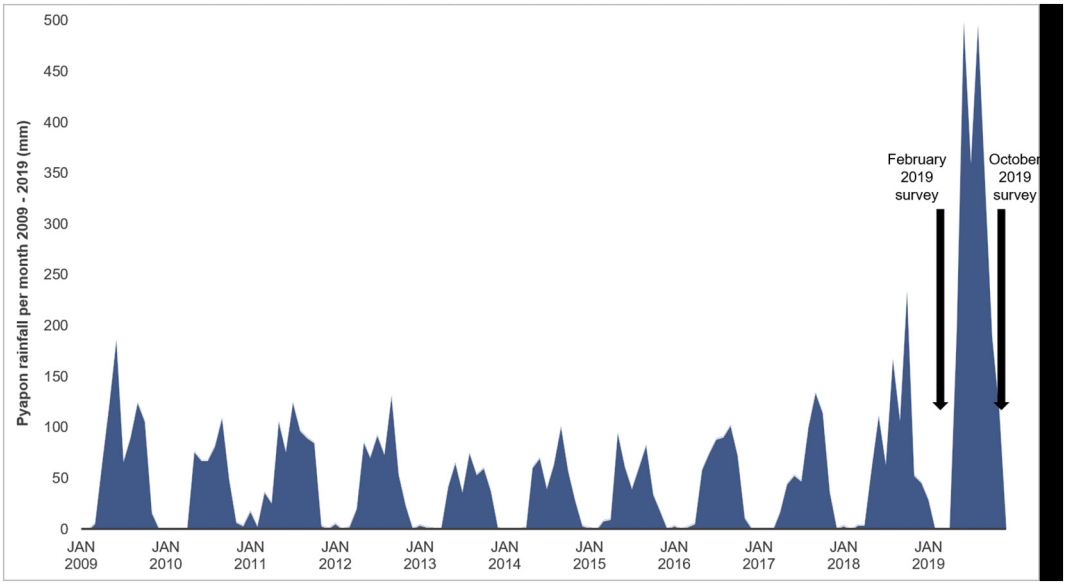

Fig. 2. Monthly precipitation in Pyapon 2009–2019. Data sourced from World Weather Online (2020).

dinitrogen gas, while the Li-Cor was calibrated using certified gas standards with concentrations of 0, 10 and 50 ppm of CH_4 in air (Gastech Australia) and 0 and 1010 ppm of CO_2 in air (Scotty Speciality Gases).

The GHG analysers were secured to a stable platform and shaded from direct radiation. Both campaigns used the same chambers and tubing, comprised of four replicate, non-absorbent transparent plastic chambers with airtight lids. These were arranged in a semi-circle around the analyser at each site and separated by no less than 1 m. Chambers were inserted to a depth of 4 cm into the substrate prior to measurement. Care was taken when installing the chambers to ensure a standard headspace volume of 1774.5 cm^3. Gases were pumped in a closed loop from the chamber to the analyser using Bev-A-Line tubing (volume 75.5 cm^3), with a small inlet inserted in the chamber lid for pressure compensation. The lid of each chamber was fitted with a small fan that ensured air was mixed within the chamber. Chambers were shaded from the sun to avoid artificially inducing thermal heating known to stimulate microbial respiration. While no emergent roots (pneumatophores, knee roots) were enclosed within chambers, underground root structures below the depth of chamber collars (4 cm) were present in sites with mangrove coverage. Autotrophic respiration (R_a) from fine root aerenchyma can be a significant component of CO_2 efflux from soils (Lovelock et al., 2006). Chambers were left to accumulate gases for between 20 and 30 min per cycle, with air samples extracted and measured by the INNOVA every 2 min while the Li-Cor measured samples continuously. At the end of each cycle, measurements resumed on the adjacent chamber within the array. GHG flux measurements were conducted over 7- and 3-day periods in February (no. observations = 92) and October respectively (no. observations = 40) during daylight hours.

Table 1
Site description and typology of the site where greenhouse gas fluxes were assessed.

Site	Description
(a) 5 year old rehabilitating forest	A replanted stand of mangroves of approximately 5 years of age at the time of sampling, dominated by *Bruguiera gymnorrhiza* and *Avicenna marina* with sporadic patches of *Nypa fruticans*. This site is located away from the main river channel and is tidally connected by feeder creeks branching of the main river channel, with tidal inundation occurring on high spring tides.
(b) 8 year old rehabilitating forest	This site was replanted approximately 8 years prior to GHG flux assessment. It is dominated by *Bruguiera gymnorrhiza*, although *Avicenna marina* and *Excoecaria agallocha* were also present along with patches of *Acanthus ilicifolius* and other herbaceous species in elevated patches. This site was adjacent to the established mangrove site on its northern border but tidal inundation is limited by the remnants of a pond wall running parallel to the river. This site was also adjacent to the DMP site, and similarly, is only fully inundated on the highest spring tides.
(c) Established riparian mangroves	Mature riverine mangroves composed predominately of *Avicennia marina* interspersed with *Nypa fruticans* on the upper banks of the river which is inundated on spring tides.
(d) Dry manky ponds	A disused, degraded dry aquaculture pond overlaying organic riverine sediments adjacent to the 8 year old rehabilitating mangrove site. A number of seedlings and saplings have recently established around the pond margins. Tidal inundation across the pond's interior is irregular and occurs only on the highest spring tides, perhaps twice a month.
(e) Partially inundated ponds	This small disused pond was tidally connected to the main river channel, although remanet walls remain in place which restricts regular tidal influx. *Acanthus ilicifolius* was present on the pond margins. This site was not assessed during the October 2019 campaign due to evidence of high levels of human disturbance.

GHG flux was calculated from a linear regression of gas concentration within the chamber over time. Only regressions with r^2 values ≥0.8 were used for flux calculations (95% of measurements from the INNOVA, 100% of measurements from the Li-Cor) from all gases and all sites following Bulmer et al. (2017).

GHG efflux rate (F_x) was calculated as:

$$Fx = (P \times V) \times \left(\frac{\Delta GHG}{\Delta t}\right)/(R \times S \times T) \quad (1)$$

where P is the initial atmospheric pressure (kPa), V is the volume of the chamber and tubing adjusted for the depth inserted into sediment (cm^3), R is the ideal gas constant (8.314 Pa m^3 K^{-1} mol^{-1}), S is the surface area covered by each chamber, T is initial air temperature (°C), and ΔGHG/Δt is the change in GHG concentration over time (Δt) based on the slope of linear regression models.

GHG efflux estimates (Mg m^2 h^{-1}) were converted to Mg CO_2e ha^{-1} y^{-1} to facilitate comparison with other published values. The N_2O and

CH_4 efflux values were multiplied by their global warming potentials of 298 and 25 respectively (Forster et al., 2007).

2.6. Soil samples

Soil carbon (C) and nitrogen (N) samples were obtained using a 50 mm diameter × 1.5 m long gouge auger (Dormer Sediment Samplers Pty Ltd, Murwillumah, NSW, Australia), with a sediment core extracted from the centre of each plot. Samples from the sediment core were taken at depth intervals of 0–10 cm, 10–50 cm, 50–100 cm and 100–150 cm. Subsamples of 10 cm in length were extracted from the mid-point of each depth interval, with the full diameter of the sediment core used. Subsamples were then oven-dried at 60 °C until a constant mass had been reached and then weighed and divided by the subsample volume to calculate dry bulk density (BD). Approximately 10 g of soil from each subsample were ground to a fine powder in a Pulverisette grinding ball mill (Fritsch, Germany) using a 25-ml milling cup lined with zirconium oxide and containing 2 × 8 mm zirconium oxide milling balls. The organic matter (OM) content of the sample was determined using the loss on ignition method with samples combusted at 550 °C for 4 h (Howard et al., 2014). 121 randomly selected samples were also analysed for %C and %N at the University of Hawaii, Hilo Analytical Laboratory using an Elemental Analyzer/Isotope Ratio Mass Spectrometry (Thermo DeltaV, Thermo Fisher Scientific, Waltham, MA, USA). Linear relationships between %C, %N and OM were established (Log %C = −1.064 + 1.497 * Log(OM); R^2 = 0.91; Log %N = −1.886 + 1.169 * Log(OM); R^2 = 0.87) from which %C and %N were estimated across all 600 samples. Depth integrated soil organic carbon and nitrogen stocks for each plot (Mg C ha^{-1}; Mg N ha^{-1}) was estimated by summing the sediment OC and N for each sediment-specific depth interval (SDI). Sediment OC was calculated as BD * SDI * %C, and a similar calculation was used to estimate depth integrated N.

2.7. Statistical analysis

We applied both a Kolmogorov – Smirnov and Shapiro – Wilk test of normality before performing logarithmic data transformation. GHG flux data was arranged based on mean values for each GHG per chamber measurement, with a three-way ANOVA applied to compare GHG flux between (a) sites in February (b) sites in October, and (c) campaigns (February dry season vs. October end of wet season 2019) using SPSS Statistics (IBM). A post – hoc Tukey honestly significant difference (HSD) was applied to identify significant differences between sites and campaigns where results showed such. The significance threshold (p) was set at 0.05 for all tests.

3. Results

3.1. GHG flux

There were clear and significant differences in GHG flux between treatments and campaigns (Fig. 3, Supplementary Information 1 and

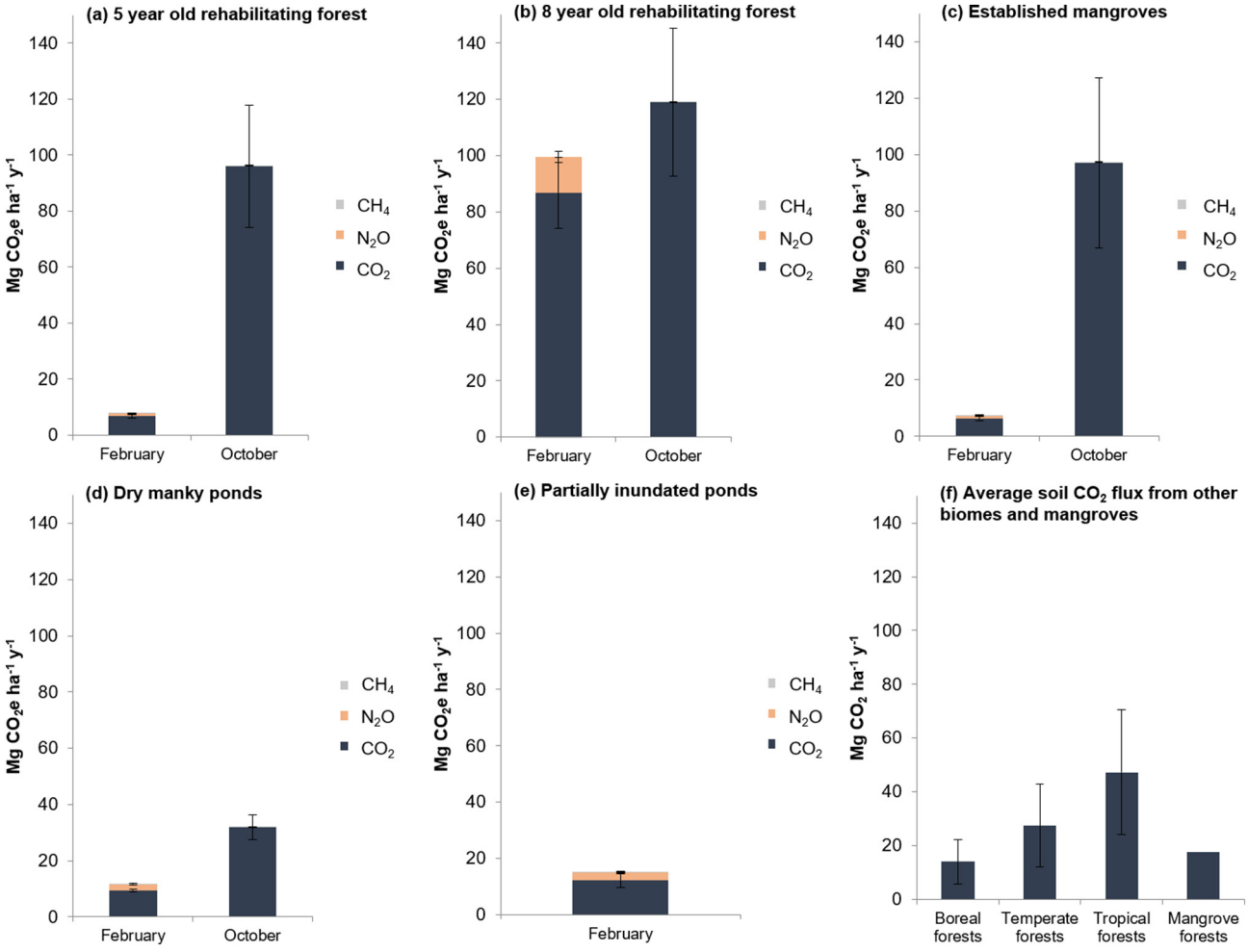

Fig. 3. Comparison of GHG flux between sites, campaigns and biomes. Data presented in Fig. 3(f) for average soil CO_2 emissions for boreal, temperate, and tropical forests sourced from Bond-Lamberty and Thomson (2010), data for mean global soil CO_2 flux from mangroves sourced from Alongi (2014). Note measurements in October were not undertaken in (e) Partially inundated ponds. Significant differences ($p \leq 0.05$) between campaigns at the same sites are denoted with an asterisk (*).

Table 2
Canopy height, density and mean tree DBH, mean above (AGB) and below (BGB) ground biomass and estimated NPP of developing mangrove forest sites, and biomass of established mangroves. Bs = *Bruguiera sexangula*, Av = *Avicennia sp.*, Ra = *Rhizophora apiculata*. Values are means plus/minus standard errors. NA is not available.

Site	Structural attributes						Biomass and productivity			
	Species dominance (%)	Canopy height (m)	Tree density (trees ha^{-1})	DBH (cm)	Seedling and sapling density (stems ha^{-1})	Basal area (m^2 ha^{-1})	AGB (Mg C ha^{-1})	BGB (Mg C ha^{-1})	Total (Mg C ha^{-1})	Estimated NPP (Mg C ha^{-1} $year^{-1}$)
5 year old rehabilitating forest	Bs (94%)	3–4 m	2, 468 ± 172	5.9 ± 0.8	71, 334 ± 9428	15 ± 2.7	19.7 ± 3.4	8 ± 1.4	27.7 ± 4.8	7.3 ± 1
8 year old rehabilitating forest	Bs (96%)	5–6 m	1, 580 ± 78	8.6 ± 0.5	45, 876 ± 18,126	19.7 ± 1.4	27.4 ± 3	11.3 ± 0.9	38.8 ± 3.9	6.4 ± 0.5
Established mangroves	Av (48%); Bs (10%); Ra (9%)	3–22 m	3415 ± 273	9.1 ± 0.5	NA	36.1 ± 5.5	121 ± 22	42 ± 7	171 ± 29	2.9 ± 0.1

2), particularly for CO_2 efflux where there are two immediately obvious results. Firstly, during the February campaign the 8 year old rehabilitating site had much higher rates of CO_2 efflux (86.8 ± 12.7 Mg CO_2e ha^{-1} yr^{-1}) than any other treatment (Fig. 3b), with the next highest CO_2 efflux of just 12.2 ± 1.8 Mg CO_2e ha^{-1} yr^{-1} (Partially inundated ponds, Fig. 3e). Secondly, during the October (extreme monsoon season) campaign all treatments had high rates of CO_2 efflux ranging between 31.9 ± 4.4 and 118.9 ± 26.3 Mg CO_2e ha^{-1} yr^{-1} for the DMP and 8 year old rehabilitating sites respectively (Fig. 3d and b). The resultant percentage increase in CO_2 efflux between February and October 2019 ranged from 37% - 1312% (8 and 5 year old rehabilitating sites respectively). During the February campaign where N_2O was measured, N_2O and CO_2 showed a strong positive correlation ($R^2 = 0.99$). Methane fluxes were very low and were a minor contribution to overall GHG flux for all sites. There was a clear trend, however, with methane efflux increasing between February and October in both rehabilitating and established mangrove sites (50–400% increase, Supplementary Information 1), although no increase was observed in the DMP. Additionally, an important observation was that while the range in CO_2 efflux between individual chambers in an array was often high (for example, a range of 203 Mg CO_2e ha^{-1} yr^{-1} between the highest and lowest CO_2 efflux recorded during incubations from different chambers at the 8 year old site during February, standard deviation = 87.1 Mg CO_2e ha^{-1} yr^{-1}), the range in CO_2 efflux in repeat measurements of the same chambers (i.e. at the same position) was typically small (e.g. an average range of 16.4 Mg CO_2e ha^{-1} yr^{-1} between the highest and lowest CO_2 efflux recorded in the same chamber at the 8 year old site during February). The consistency in measurements from the same chambers reflects the highly heterogenous nature of mangrove soil CO_2 effluxes, particularly given chambers in an array were separated by only 1 m.

3.2. Structural attributes, biomass, and estimated NPP of developing mangrove forests

Structural attributes of the two rehabilitating sites showed differences characteristic of age in developing mangrove forests, with the older, 8 year old planted mangroves exhibiting lower tree and seedling densities but higher DBH, basal area, and canopy height than the 5 year old site (Table 2). However, while overall biomass of the 8 year old site (38.8 ± 3.9 Mg C ha^{-1}) was, higher than the younger site (27.7 ± 4.8 Mg C ha^{-1}), when results are scaled to estimates of NPP (inclusive of estimated leaf litter production) the younger site was accumulating biomass at a slightly higher rate of 7.3 ± 1 Mg C ha^{-1} yr^{-1} compared to 6.4 ± 0.5 Mg C ha^{-1} yr^{-1} in the 8 year old site. While NPP of both developing forests was higher than the established mangroves (2.9 ± 0.1 Mg C ha^{-1} yr^{-1}), basal area (36.1 ± 5.5 m^2 ha^{-1}) was much greater as is expected of more developed, mature forests.

3.3. Soil characteristics

Soil characteristics (BD, C%, N%) were relatively homogenous across the Ayeyarwady Delta with little difference between natural mangroves, regenerating mangroves, or aquaculture ponds (Table 3). Total soil carbon was slightly lower in aquaculture ponds than in natural and regenerating mangrove sites by 14 and 34 Mg C ha^{-1} respectively. Total soil nitrogen was also similar among different land-uses.

4. Discussion

Soil-atmosphere GHG efflux rates from the 8 year old rehabilitating mangrove site in February and all treatments assessed during October were among the highest values yet recorded from any mangrove ecosystem using the in-situ chamber technique (Table 4). While CO_2 efflux in February from the 5 year old and established mangrove sites were similar to global averages reported for healthy mangrove ecosystems (range 9.6 ± 7.2–17.6 Mg CO_2 ha^{-1} yr^{-1}, Bouillon et al., 2008 and Alongi, 2014 respectively), flux from the 8 year old site in February and October was 45–98% higher than previously reported maxima (59.9 Mg CO_2 ha^{-1} yr^{-1}, Kristensen et al., 2008), and much higher than mean soil CO_2 emissions from other biomes (Fig. 3f). The high rates of CO_2 efflux are, however, consistent with inferred potential fluxes estimated from high rates of fine root turnover (Robertson and Alongi, 2016). The N_2O flux from this forest in February (12.8 ± 1.9 Mg CO_2e ha^{-1} yr^{-1}) was also among the highest recorded from mangroves (range − 1.08–15.8 Mg CO_2e ha^{-1} yr^{-1}; Alongi, 2009. Table 4). While methane production increased substantially during the wet season (October), the overall contribution to GHG fluxes remained very low and below the global median for mangrove ecosystems of 0.41 Mg CO_2e ha^{-1} yr^{-1} (Al-Haj and Fulweiler, 2020).

Table 3
Summary of soil properties measured to 1 m soil depth (mean ± standard error).

Land-use	No. soil samples	Mean bulk density (g cm^{-3})	Mean carbon content (%)	Total carbon stock (Mg C ha^{-1})	N content (%)	Total N stock (Mg N ha^{-1})
Natural mangroves	36	0.851 ± 0.017	1.97 ± 0.11	158 ± 13	0.146 ± 0.006	13.3 ± 1.2
Regenerating mangroves	33	0.873 ± 0.016	2.04 ± 0.13	177 ± 17	0.148 ± 0.007	11.9 ± 0.8
Aquaculture ponds	20	0.867 ± 0.023	1.84 ± 0.10	144 ± 15	0.170 ± 0.030	11.1 ± 0.9

Table 4
Comparison of selected published estimates of CO_2, CH_4 and N_2O emissions from mangrove soils using in-situ gas exchange/chamber measurements as a function of landuse. Values for reported N_2O and CH_4 emissions are multiplied by their global warming potentials of 298 and 25 respectively (Forster et al., 2007). Exposed = sediment – atmosphere emissions, inundated = water – atmosphere emissions. The range in measurements is included in parenthesis where applicable. Negative values indicate overall C sequestration. Ra = *R. stylosa*; Ct = *C. tagal*; Ra = *R. apiculata*; Bg = *B. gymnorrhiza*; Sa = *S. alba*, Am = *Avicenna marina*, Kc = *K. obovate*, Aa = *Avicennia alba*, Ao = *Avicennia officinalis*, Rm = *Rhizophora mucronata*. N/D = not detected.

Location	Site conditions/notes	GHG flux (Mg CO_2e ha^{-1} yr^{-1})			Total GHG flux	Data source
		CO_2	N_2O	CH_4		
Intact, established mangroves						
Ayeyarwady Delta, Myanmar	Dry season (February)	8 ± 0.5	1.6 ± 0.3	0.2 ± 0.1	9.8 ± 0.9	This study
	Wet season (October)	78.5 ± 16.2	N/A	0.3 ± 0.1	78.8 ± 16.3	
South Sulawesi, Indonesia (Ref 1_{TI})	*Ra*/*Sa*/*Bg* dominated site	16.7 ± 0.8	1.3 ± 0.1	1.4 ± 0.2	19.4 ± 1.1	Cameron et al. (2019a)
North Sulawesi, Indonesia (Ref 2_{TW})	*Ct* dominated site	28 ± 2.3	4 ± 0.5	0.4 ± 0.2	32.4 ± 3	Cameron et al. (2019a)
North Island, New Zealand	*Am*, Exposed, biofilm intact	27.1 ± 7.4			27.1 ± 7.4	Bulmer et al. (2015)
Whangamata Harbour, New Zealand	*Am*, Exposed, summer	12.8 ± 1.5			12.8 ± 1.5	Bulmer et al. (2017)
	Am, Exposed, winter	4.3 ± 1.2			4.3 ± 1.2	
Honda Bay, Philippines	*R.* spp., Undisturbed natural mangroves	40.3 ± 3.8			40.3 ± 3.8	Castillo et al. (2017)
New Caledonia	*R.* spp., semi-arid	14.7		0.2	14.9	Jacotot et al. (2019)
Red Sea coastline, Saudi Arabia	Reported diel range from arid mangroves	−13.9–30.1		0–0.02	−13.9–30.12	Sea et al. (2018)
Perancak estuary, Bali, Indonesia	Aa, Ao, Am, Rs, Rm, Ra, Sa, Bg	44.8 ± 6.6			44.8 ± 6.6	Sidik et al. (2019)
Chwaka Bay, Tanzania	*Rm*, *Am*, *Ct*, *Bg*, Undisturbed natural mangroves	58.8			58.8	Gillis et al. (2017)
Southern Moreton Bay, Queensland, Australia	Exposed (soil emissions)	9.8	0.1	0.1	10	Maher et al. (2018)
Global average estimates for mangroves	Sum of autotrophic and heterotrophic respiration, CO_2	17.6		1.9	19.5	Alongi (2014)
	Exposed	26.3 (2.3–59.9)			26.3	Kristensen et al. (2008)
	Inundated	8.2 (1.6–19.4)			8.2	
	Median value reported			0.4		Al-Haj and Fulweiler (2020)
		9.1 ± 1.4			9.1 ± 1.4	Rosentreter et al. (2018)
Aquaculture ponds						
Ayeyarwady Delta, Myanmar	DMP, dry season	9.4 ± 0.6	2.2 ± 0.3	0.1 ± 0.2	11.7 ± 1.1	This study
	DMP, wet season	31.9 ± 4.4	N/A	0.1 ± 0.0	32 ± 4.4	
	Partially inundated ponds, dry season	12.2 ± 2.7	2.7 ± 3.2	0.3 ± 1	15.2 ± 6.9	
South Sulawesi, Indonesia	Inundated, operating ponds	0.5 ± 0.0	N/D	0.6 ± 0.3	1.1 ± 0.2	Cameron et al. (2019a)
South Sulawesi, Indonesia	Exposed, no hydrological connectivity, biofilm intact	25.6 ± 1.6	2.6 ± 0.3	2.5 ± 0.2	30.6 ± 1.9	Cameron et al. (2019a)
North Sulawesi, Indonesia	Partially hydrologically connected, biofilm intact	11.3 ± 0.6	2.7 ± 0.3	0.5 ± 1.7	14.5 ± 2.6	Cameron et al. (2019a)
Perancak estuary, Bali, Indonesia	Abandoned pond 'walls'	43.7			43.7	Sidik and Lovelock (2013)
	Abandoned pond 'floor'. Biofilm removed.	16			16	
Honda Bay, Philippines	Abandoned ponds, little regrowth	15.9 ± 3.7			15.9 ± 3.7	Castillo et al. (2017a)
Queensland, Australia	Inundated ponds	17.5			17.5	Burford and Longmore (2001)
Worldwide (n = 233)	Operating ponds	−5.5 ± 3.3			−5.5 ± 3.3	Boyd et al. (2010)
Rehabilitating mangroves						
Ayeyarwady Delta, Myanmar	5 year old site, dry season (February)	6.5 ± 0.9	0.9 ± 0.4	0.1 ± 0.2	7.4 ± 1.4	This study
	5 year old site, wet season (October)	97.1 ± 30.2	N/A	0.4 ± 0.2	97.5 ± 30.3	
	8 year old site, dry season (February)	86.8 ± 17	12.8 ± 2.5	−0.7 ± 0.8	98.9 ± 20.2	
	8 year old site, wet season (October)	118.9 ± 24.3	N/A	0.2 ± 0.1	119.1 ± 24.4	
North Sulawesi, Indonesia	High mangrove coverage Ct, Ra, Sa, 10 years old (average of three sites)	25.7 ± 2	3.1 ± 0.5	0.7 ± 0.3	29.5 ± 2.8	Cameron et al. (2019a)
Perancak estuary, Bali, Indonesia	Aa, Ao, Am, Rs, Rm, Ra, Sa, Bg	26.8 ± 5.9			26.8 ± 5.9	Sidik et al. (2019)
Northern Vietnam	High mangrove coverage, 16 year old stand, biofilm intact	10.7 ± 4.1			10.7 ± 4.1	Grellier et al. (2017)
	High mangrove coverage, 16 year old stand, biofilm removed	16.1 ± 5.3			16.1 ± 5.3	
Northern Vietnam	High mangrove coverage, *Kc* dominated site, mean values 18 year old replanted site	15.3 ± 14.3			15.3 ± 14.3	Hien et al. (2018)
	High mangrove coverage, *Kc* dominated site, mean values 18 year old replanted site: *Wet season*	22.6 ± 17.6			22.6 ± 17.6	
	High mangrove coverage, *Kc* dominated site, mean values 18 year old replanted site: *Dry season*	8.1 ± 5.1			8.1 ± 5.1	

The high CO_2 and N_2O emissions observed from the 8 year old forest during February was most likely related to high rates of primary production whereby developing mangroves allocate high proportions of fixed carbon to roots which subsequently turnover, forming a detrital carbon substrate for microbes (Robertson and Alongi, 2016; Sidik et al., 2019). The high rates of CO_2 efflux observed at all sites, and comparatively higher rates of CH_4 emissions from vegetated sites, during the October wet season are most likely indicative of elevated rates of respiration from both mangroves and microbes as a result of high rainfall, flooding and allochthonous sediment deposition due to the extreme 2019 monsoon season (Fig. 2). Additionally, the higher CO_2 efflux observed in sites occupied by mangroves compared to unvegetated ponds (DMP site) during October is consistent with expectations that organic matter inputs and autochthonous respiration increases overall CO_2 flux.

4.1. GHG efflux during the February dry season

Mangrove vegetation development and the rate of biomass accumulation is typically nonlinear, with some studies indicating that mangroves accumulate biomass most rapidly between 6 and 10 years old (Komiyama et al., 2008; Kridiborworn et al., 2012). This phenomenon, possibly combined with increased productivity due to lower salinity as a legacy of higher than usual rainfall associated with the 2018 monsoonal season (Fig. 2), could well have underpinned elevated CO_2 efflux at the 8 year old site. Some mangroves, particularly those growing under conditions of elevated soil salinity concentrations (e.g. landward associations and scrub mangroves) or depleted nutrient settings, have been shown to significantly invest in belowground biomass as a means to accumulate, conserve and recycle nutrients (Alongi, 2009; Komiyama et al., 1987). Investment of a high proportion of new growth in belowground biomass is also consistent with several recent observations in developing restored mangroves forests of South East Asia (e.g. Poungparn et al., 2016; Muhammad-Nor et al., 2019; Sidik et al., 2019) as well as tropical Australia (Robertson and Alongi, 2016).

Consistent with the high seasonal variation in CO_2 efflux observed in this study, mangrove root production is also highly seasonal. Poungparn et al. (2016), for instance, recorded highest root productivity during the wet and early cool dry season for secondary mangrove forests in Thailand (our observations were recorded in the middle of the dry season in February and end of the wet season in October). This suggests increased rainfall and a reduction in porewater salinity stimulates root growth (Muhammad-Nor et al., 2019) and thus respiration. Terrestrial forests show similar patterns, with seasonal root production in tropical species such as rubber trees directly correlating to rainfall (Maeght et al., 2015). Additionally, Adame et al. (2017) found that root biomass tends to be higher in dense mangrove forests with small DBH and high interstitial salinity. These factors also influence both replanted sites where density is comparatively high and DBH small, while as noted in Table 1, these sites are also irregularly inundated which results in elevated soil salinity.

The accumulation of dead fine roots over time elevates concentrations of carbon and nitrogen and forms a labile carbon supply more easily absorbed via digestion by the microbiota associated with plant roots and soils, rather than leaf litter or allochthonous carbon (Robertson and Alongi, 2016; Girkin et al., 2018; Cameron et al., 2019b; Malhi et al., 2011; Lovelock, 2008). Additionally, living fine roots either respire CO_2 directly into surrounding soils, or else form a constituent carbon source for the production of root exudates which then leach into soils (Cameron et al., 2019a, 2019b, Lovelock, 2008). These processes may facilitate a significant build-up of labile soil organic matter, forming a large substrate availability and subsequent increase in soil microbial populations (Alongi and Robertson, 2016). Decomposition, in turn, releases essential nutrients back into the soil for plant uptake, with heterotrophic respiration (CO_2) and the breakdown of nitrogen subsequently reaching the soil surface and exchanging with the atmosphere. Resultant CO_2 efflux rates from the decomposition of dead fine roots can be considerable, with Robertson and Alongi (2016) estimating carbon fluxes via this mechanism ranging from 33.5–251.8 Mg CO_2 ha^{-1} yr^{-1} from mangrove forests on Hinchinbrook Island, northeastern Australia. Additionally, soil organic matter decomposition rates can accelerate substantially in the presence of plant roots, and this mechanism – termed the rhizophore priming effect (Keuper et al., 2020) - may be particularly pronounced in the 8 year old rehabilitating site. While heterotrophic respiration typically comprises between 40 and 60% of soil CO_2 flux in mangrove forests (see studies by Castillo et al., 2017, Gillis et al., 2017, Hien et al., 2018, and Lang'at et al., 2014), it has been recorded as high as 79.5% of total CO_2 efflux in temperate mangroves in New Zealand (Bulmer et al., 2017). Similarly, high rates of CO_2 efflux from the 8 year old rehabilitating site in February may also indicate contributions from high levels of heterotrophic respiration.

The successional stage of mangrove stands is also likely to influence rates of CO_2 efflux (Pregitzer and Euskirchen, 2004). Estimated NPP (carbon fixation) of the 8 year old developing forest (when converted to CO_2) was only 23.5 $\pm$ 1.8 Mg CO_2e ha^{-1} yr^{-1}. This is at the lower end of the average rate of biomass accumulation in 6–10 year old coastal fringing and estuarine mangrove forests (32.8 Mg CO_2e ha^{-1} yr^{-1}) following interpolations of data reported in Cameron et al. (2018). When the amount of fixed carbon is compared to our soil GHG efflux results for February (and October), the 8 year old mangrove would be a significant net source of carbon to the atmosphere if efflux remained constant year round. While this is consistent with observations in developing boreal and temperate forests (0–10 years of age), which have been estimated to be net sources of 0.4 and 7 Mg CO_2 ha^{-1} yr^{-1} respectively (Pregitzer and Euskirchen, 2004), net CO_2 emissions from the 8 year old site are an order of magnitude greater. In contrast, while NPP in the younger, 5 year old replanted site was slightly higher than the 8 year old site, it may not have reached the stage where growth spurts and high rates of biomass allocation to fine roots become evident. Additionally, although it was in close proximity to the 8 year old rehabilitation site, the 5 year old site may have a slightly different inundation regime and soil conditions which may also limit growth, allocation of carbon to roots or the proportion of CO_2 efflux from the surface compared to that exported laterally. Soil CO_2 efflux also tends to decline in mature, established forests (Pregitzer and Euskirchen, 2004), which may partially explain why CO_2 efflux was lower in the established mangrove site compared to the rehabilitating sites, although other environmental factors may also contribute. Furthermore, soil CO_2 efflux from the ponds, established mangroves and the 5 year old rehabilitating site in February were similar to mean dry season CO_2 efflux reported from comparable deltaic mangrove ecosystems overlaying mineral soils in Northern Vietnam (8.1 $\pm$ 5.1 Mg CO_2 ha^{-1} yr^{-1}, Hien et al., 2018. See Table 4). It is probable, therefore, that CO_2 efflux from the 8 year old developing forest would not be sustained at such high rates in the long-term and would eventually level off to rates observed in established forests, with carbon accumulation in soils and biomass counteracting net losses. While there is a growing understanding of changes in carbon stocks over natural and rehabilitating mangrove chronosequences (e.g. Marchand, 2017; Cameron et al., 2018; and Walcker et al., 2018), these results also signal a clear research prerogative to better understand carbon dynamics and the relationship between CO_2 flux and carbon fixation during mangrove forest development.

4.2. GHG efflux during the October end of wet season

The extremely high rainfall and flooding associated with the 2019 monsoon season is likely the key factor driving high rates of CO_2 emissions from all sites during October. Precipitation events are known to lead to substantial short-term increases in respiration rates as soils cycle between dry and wet conditions under a phenomenon known as the 'Birch effect' (Fernandez-Bou et al., 2020). Freshwater influx from

rainfall, flooded rivers, and surface water runoff, along with hydroperiod and groundwater infiltration, all influence moisture content and salinity within mangrove soils. This, in turn, can influence key process such as (a) the diffusion of organic molecules in soils and subsequent mobilisation of carbon (b) the rate of soil organic matter decomposition by heterotrophs, and (c) primary production (Phillips and Nickerson, 2015; Fernandez-Bou et al., 2020), all of which influence GHG flux in mangroves. Higher soil water content, as typically occurs in the saturated soils of seaward mangroves under longer hydroperiods (Cameron et al., 2019a, 2019b) or through rainfall and surface flooding, can break down soil microstructures and release labile organic matter in soils (desorption) and enhance microbial consumption (Spivak et al., 2019; Fernandez-Bou et al., 2020) leading to higher rates of heterotrophic CO_2 flux. Similar seasonal variations have also been recorded from deltaic systems in Northern Vietnam, where soil-atmosphere CO_2 flux increased by 174% during the wet season (Hien et al., 2018), while Koné and Borges (2008) and Linto et al. (2014) also observed 5 and 2–5 fold increases in water – air efflux during the wet season from mangroves in Kien Vang (Vietnam) and the Andaman Islands respectively. Additionally, the deposition of alluvium during flooding events is also likely to form a mineral rich nutrient source for microbial communities as well as stimulate plant growth and productivity, a phenomenon also seen following storm surges (Krauss and Osland, 2019).

Salinity is another key factor regulating both the decomposition of organic soil matter and rates of production in mangroves. Freshwater influx lowers salinity of porewater and promotes key physiological process such as photosynthesis and evapotranspiration in mangroves (López-Medellín and Ezcurra, 2012; Ochoa-Gómez et al., 2019). Additionally, lowered porewater salinity reduces osmotic stress and the build-up of ions toxic to microbes in soils (Elmajdoub and Marschner, 2015), thereby enhancing metabolic activity and subsequent autotrophic and heterotrophic respiration. Salinity is considered the most important factor controlling CH_4 release (Poffenbarger et al., 2011), with freshwater reducing sulphate reduction and creating more favourable conditions for methane producing bacteria (methanogens) over methane consuming bacteria (methanotrophs), which is likely why methane emissions were also significantly higher in October than February. Over annual timescales, soil respiration also tends to correlate with seasonal patterns in soil moisture and temperature (Phillips and Nickerson, 2015), peaking during warm and moist periods (i.e. October) and declining in cooler, drier conditions (i.e. February). Fluxes from the soil surface may also dominate where the lateral export of CO_2 into adjacent waters from tidal forcing is limited by infrequent tidal inundation, particularly in compact sediments where preferential pathways for diffusion are few (Alongi, 2014; Maher et al., 2018) as occurred at our sites.

4.3. Soil properties and GHG efflux

Mangrove soils in the Ayeyarwady Delta had similar characteristics to other deltaic settings. Soil carbon stocks, for instance, were similar to those reported from a study also conducted in the Ayeyarwady Delta (167 ± 58 Mg C ha^{-1}, top 1 m of soil. Thant et al., 2012), Bangladesh (Sundarbans Delta, range for the top 1 m of soil 90–134.2 Mg C ha^{-1}. Rahman et al., 2015) and Vietnam (Mekong Delta, 272.3 Mg C ha^{-1} for fringing mangroves to 1 m depth. Nam et al., 2016; Red River Delta, 159.6 ± 4 Mg C ha^{-1}, top 1 m of soil. Ha et al., 2018) and were consistent with modelled mangrove soil carbon data for the wider region (Sanderman et al., 2018). Soil carbon stocks in all of these mineral deltaic settings are comparatively low compared to the global average for mangroves to 1 m depth of 361 Mg C ha^{-1} (Sanderman et al., 2018), which is 184–217 Mg C ha^{-1} more than our sites. Low carbon stocks and homogeneity in soil characteristics among natural mangroves, regenerating mangroves and aquaculture ponds likely reflects high levels of sediment deposition from the Ayeyarwady River which effectively dilutes organic matter and hence carbon content as more mineral, alluvial sediment derived from eroded material in the upper catchment accumulates over time. Slightly lower levels of soil carbon in aquaculture ponds, although not significantly different from mangrove sites, likely reflect reduced autochthonous organic matter inputs and higher levels of heterotrophy (Sidik and Lovelock, 2013).

The relative homogeneity in soil characteristics, such as carbon and nitrogen concentrations, across the study site implies these are not decisive factors influencing GHG flux between sites. However, we observed high spatial and temporal heterogeneity in soil GHG efflux, with substantial variance observed at sites both between measurements taken from the same chambers at the same site as well as seasonally. This is probably related to heterotrophic respiration from highly localised, dense populations of soil microbes concentrated around substrate repositories which are formed by a large mass of high fine root turnover in the 8 year old developing forest (October), and elevated rainfall releasing organic nutrients via hydrolysis stimulating both autotrophic and heterotrophic respiration (February). These results serve to highlight the complex interactions among biophysical variables influencing GHG flux, which - particularly in mangrove ecosystems - display high temporal and spatial heterogeneity and may even differ within the same forest over time (Alongi, 2009).

Although our results represent a short-term assessment of flux dynamics, inclusive of an extreme monsoonal event, they serve to highlight the critical importance of assessing GHG flux in-situ in order to quantify variability in GHG dynamics over time. Scaling fluxes spatially, temporally and under changing land uses using the static chamber technique is challenging due to high spatial and temporal variation, particularly in rehabilitating mangroves in areas with pronounced seasonal variations in conditions. Methods such as eddy covariance, which integrate spatial and temporal variability of gas exchange in sites with adequate fetch, provide robust models (Lu et al., 2017) but are also more expensive, resource intensive and difficult to deploy in regions such as the Ayeyarwady Delta.

5. Conclusions

While the 8 year old developing forest in February and all sites during October had high levels of soil CO_2 efflux, in the long-term these episodic high rates of CO_2 efflux are likely to be counterbalanced by carbon sequestration in soils and biomass as mangroves regrow. While this observation is consistent with prevailing evidence suggesting mangroves are overall net carbon sinks, not sources (Alongi, 2014), the current study also highlights profound implications for determining the extent of long-term carbon storage and sequestration in Myanmar. Not only does Myanmar continue to exhibit among the highest rates of mangrove loss and conversion in the world (Goldberg et al., 2020) resulting in substantial carbon emissions (Friess et al., 2020), but climate change is also likely to increase the severity and intensity of extreme rainfall events in SE Asia (Loo et al., 2015). As seen in the current study, this may substantially increase short-term emissions and therefore counter-balance carbon sequestration gains. Additionally, methane fluxes were low across seasons, consistent with observations from other mangrove ecosystems. Further work is needed to more accurately quantify such emissions, which are an important aspect when developing forest carbon offset projects involving the restoration of mangrove ecosystems.

CRediT authorship contribution statement

Clint Cameron: Conceptualization, Methodology, Formal analysis, Writing - original draft. **Lindsay B. Hutley:** Conceptualization, Methodology, Writing - review & editing. **Niels C. Munksgaard:** Conceptualization, Methodology, Writing - review & editing. **Sang Phan:** Formal analysis, Project administration, Writing - review & editing. **Toe Aung:** Project administration, Writing - review & editing. **Thinn Thinn:** Project administration, Writing - review & editing. **Win Maung Aye:** Project administration, Writing - review & editing. **Catherine E. Lovelock:** Project

administration, Formal analysis, Writing - original draft, Writing - review & editing.

Declaration of competing interest

The authors declare that they have no known competing financial interests or personal relationships that could have appeared to influence the work reported in this paper.

Acknowledgements

This research was generously supported by UNEP Grid-Arendal as part of the Global Environment Fund project 'Standardised Methodologies for Carbon Accounting and Ecosystem Services Valuation of Blue Forests' and the Asia-Pacific Network for Sustainable Forest Management (2018P1-MYR-03). Thanks to Michael Bird (James Cook University) for the use of the INNOVA 1412i analyser, and the Research Institute for the Environment and Livelihoods (Charles Darwin University) for use of the Li-Cor analyser. Thanks to Dr. Nyi Nyi Kyaw, Director General of the Forest Department of Myanmar, and the Forest Department of Myanmar for their support.

Appendix A. Supplementary data

Supplementary data to this article can be found online at https://doi.org/10.1016/j.scitotenv.2020.143422.

References

Adame, M.F., Cherian, S., Reef, R., Stewart-Koster, B., 2017. Mangrove root biomass and the uncertainty of belowground carbon estimations. For. Ecol. Manag. 403, 52–60.

Al-Haj, A.N., Fulweiler, R.W., 2020. A synthesis of methane emissions from shallow vegetated coastal ecosystems. Glob. Chang. Biol. 26 (5), 2988–3005 10.111/gcb.15046.

Alongi, D.M., 2009. The Energetics of Mangrove Forests. Springer Science & Business Media, New York, USA.

Alongi, D.M., 2014. Carbon cycling and storage in mangrove forests. Annu. Rev. Mar. Sci. 6, 195–219.

Asia-Pacific Network for Sustainable Forest Management and Rehabilitation (APFNet), 2017. Integrated planning and practises for mangrove management associated with agriculture and aquaculture in Myanmar (2017PI-MYR). Project Document published by the Forestry Department of Myanmar and the Department of Agriculture and Water Resources, Australia 56pp.

Bond-Lamberty, B., Thomson, A., 2010. A global database of soil CO_2 respiration data. Biogeosciences 7 (6).

Bouillon, S., Borges, A.V., Castañeda-Moya, E., Diele, K., Dittmar, T., Duke, N.C., Middelburg, J.J., 2008. Mangrove production and carbon sinks: a revision of global budget estimates. Glob. Biogeochem. Cycles 22 (2).

Boyd, C.E., Wood, C.W., Chaney, P.L., Queiroz, J.F., 2010. Role of aquaculture pond sediments in sequestration of annual global carbon emissions. Environ. Pollut. 158 (8), 2537–2540. https://doi.org/10.1016/j.envpol.2010.04.025.

Bulmer, R.H., Lundquist, C., Schwendenmann, L., 2015. Sediment properties and CO_2 efflux from intact and cleared temperate mangrove forests. Biogeosciences 12 (20), 6169.

Bulmer, R.H., Schwendenmann, L., Lohrer, A.M., Lundquist, C.J., 2017. Sediment carbon and nutrient fluxes from cleared and intact temperate mangrove ecosystems and adjacent sandflats. Sci. Total Environ. 599, 1874–1884.

Burford, M.A., Longmore, A.R., 2001. High ammonium production from sediments in hypereutrophic shrimp ponds. Mar. Ecol. Prog. Ser. 224, 187–195.

Cameron, C., Hutley, L.B., Friess, D.A., Brown, B., 2018. Community structure dynamics and carbon stock change of rehabilitated mangrove forests in Sulawesi, Indonesia. Ecol. Appl. 29 (1), e01810.

Cameron, C., Hutley, L.B., Friess, D.A., Munksgaard, N.C., 2019a. Hydroperiod, soil moisture and bioturbation are critical drivers of greenhouse gas fluxes and vary as a function of landuse change in mangroves of Sulawesi, Indonesia. Sci. Total Environ. 654, 365–377.

Cameron, C., Hutley, L.B., Friess, D.A., 2019b. Estimating the full greenhouse gas emissions offset potential and profile between rehabilitating and established mangroves. Sci. Total Environ. 665, 419–431.

Castillo, J.A.A., Apan, A.A., Maraseni, T.N., Salmo III, S.G., 2017. Soil greenhouse gas fluxes in tropical mangrove forests and in land uses on deforested mangrove lands. Catena 15.

Elmajdoub, B., Marschner, P., 2015. Response of microbial activity and biomass to soil salinity when supplied with glucose and cellulose. J. Soil Sci. Plant Nutr. 15 (4), 816–832.

Estoque, R.C., Myint, S.W., Wang, C., Ishtiaque, A., Aung, T.T., Emerton, L., Fan, C., 2018. Assessing environmental impacts and change in Myanmar's mangrove ecosystem service value due to deforestation (2000–2014). Glob. Chang. Biol. 24 (11), 5391–5410.

Fernandez-Bou, A.S., Dierick, D., Allen, M.F., Harmon, T.C., 2020. Precipitation-drainage cycles lead to hot moments in soil carbon dioxide dynamics in a Neotropical wet forest. Glob. Chang. Biol. 26 (9), 5303–5319.

Forster, P., Ramaswamy, V., Artaxo, P., Berntsen, T., Betts, R., Fahey, D.W., Myhre, G., 2007. Changes in atmospheric constituents and in radiative forcing. Chapter 2 Climate Change 2007. The Physical Science Basis.

Friess, D.A., Krauss, K.W., Taillardat, P., Adame, M.F., Yando, E.S., Cameron, C., Sasmito, S.D, Sillanpää, M., 2020. Mangrove Blue Carbon in the Face of Deforestation, Climate Change, and Restoration. Annual Plant Reviews online. pp. 427–456.

Gillis, L., Belshe, E., Narayan, G., 2017. Deforested mangroves affect the potential for carbon linkages between connected ecosystems. Estuar. Coasts 40 (4), 1207–1213.

Girkin, N.T., Turner, B.L., Ostle, N., Craigon, J., Sjögersten, S., 2018. Root exudate analogues accelerate CO_2 and CH_4 production in tropical peat. Soil Biol. Biochem. 117, 48–55.

Goldberg, L., Lagomasino, D., Thomas, N., Fatoyinbo, T., 2020. Global declines in human-driven mangrove loss. Glob. Chang. Biol. https://doi.org/10.1111/gcb.15275.

Green Growth Knowledge Partnership, 2020. Economic Appraisal of Ayeyarwady Delta Mangrove Forests. Global Green Growth Institute, Seoul 68 p.

Grellier, S., Janeau, J.-L., Hoai, N.D., Kim, C.N.T., Phuong, Q.L.T., Thu, T.P.T., Marchand, C., 2017. Changes in soil characteristics and C dynamics after mangrove clearing (Vietnam). Sci. Total Environ. 593, 654–663.

Ha, T.H., Marchand, C., Aimé, J., Dang, H.N., Phan, N.H., Nguyen, X.T., Nguyen, T.K.C., 2018. Belowground carbon sequestration in a mature planted mangroves (Northern Viet Nam). For. Ecol. Manag. 407, 191–199.

Hamilton, S.E., Casey, D., 2016. Creation of a high spatio-temporal resolution global database of continuous mangrove forest cover for the 21st century (CGMFC-21). Glob. Ecol. Biogeogr. 25, 729–738.

Hien, H.T., Marchand, C., Aimé, J., Cuc, N.T.K., 2018. Seasonal variability of CO_2 emissions from sediments in planted mangroves (Northern Viet Nam). Estuar. Coast. Shelf Sci. 213, 28–39.

Howard, J., Hoyt, S., Isensee, K., Telszewski, M., Pidgeon, E., 2014. Coastal Blue Carbon: Methods for Assessing Carbon Stocks and Emissions Factors in Mangroves, Tidal Salt Marshes, and Seagrasses. Conservation International, Intergovernmental Oceanographic Commission of UNESCO, International Union for Conservation of Nature, Arlington, Virginia, USA, Arlington, VA, USA.

International Federation of the Red Cross, 2019. Myanmar: Monsoon Floods 2019. DREF Final Report. https://reliefweb.int/report/myanmar/myanmar-monsoon-floods-2019-dref-n-mdrmm012-final-report.

Jacotot, A., Marchand, C., Allenbach, M., 2019. Biofilm and temperature controls on greenhouse gas (CO_2 and CH_4) emissions from a Rhizophora mangrove soil (New Caledonia). Sci. Total Environ. 650, 1019–1028.

Kauffman, J.B., Donato, D.C., 2012. Protocols for the Measurement, Monitoring and Reporting of Structure, Biomass, and Carbon Stocks in Mangrove Forests. CIFOR, Bogor, Indonesia.

Kauffman, J.B., Heider, C., Norfolk, J., Payton, F., 2014. Carbon stocks of intact mangroves and carbon emissions arising from their conversion in the Dominican Republic. Ecol. Appl. 24 (3), 518–527.

Keuper, F., Wild, B., Kummu, M., Beer, C., Blume-Werry, G., Fontaine, S., Jalava, M., 2020. Carbon loss from northern circumpolar permafrost soils amplified by rhizosphere priming. Nature Geoscience 1–6.

Komiyama, A., Ogino, K., Aksornkoae, S., Sabhasri, S., 1987. Root biomass of a mangrove forest in southern Thailand. 1. Estimation by the trench method and the zonal structure of root biomass. J. Trop. Ecol. 3 (2), 97–108.

Komiyama, A., Poungparn, S., Kato, S., 2005. Common allometric equations for estimating the tree weight of mangroves. J. Trop. Ecol. 21 (4), 471–477.

Komiyama, A., Ong, J.E., Poungparn, S., 2008. Allometry, biomass, and productivity of mangrove forests: a review. Aquat. Bot. 89 (2), 128–137.

Koné, Y.M., Borges, A.V., 2008. Dissolved inorganic carbon dynamics in the waters surrounding forested mangroves of the Ca Mau Province (Vietnam). Estuar. Coast. Shelf Sci. 77 (3), 409–421.

Krauss, K.W., Osland, M.J., 2019. Tropical cyclones and the organization of mangrove forests: a review. Ann. Bot. 125 (2), 213–234.

Kridiborworn, P., Chidthaisong, A., Yuttitham, M., Tripetchkul, S., 2012. Carbon sequestration by mangrove forest planted specifically for charcoal production in Yeesarn, Samut Songkram. Journal of Sustainable Energy & Environment 3 (2), 87–92.

Kristensen, E., Bouillon, S., Dittmar, T., Marchand, C., 2008. Organic carbon dynamics in mangrove ecosystems: a review. Aquat. Bot. 89 (2), 201–219.

Lang'at, J.K.S., Kairo, J.G., Mencuccini, M., Bouillon, S., Skov, M.W., Waldron, S., Huxham, M., 2014. Rapid losses of surface elevation following tree girdling and cutting in tropical mangroves. (research article). PLoS One 9 (9).

Linto, N., Barnes, J., Ramachandran, R., Divia, J., Ramachandran, P., Upstill-Goddard, R.C., 2014. Carbon dioxide and methane emissions from mangrove-associated waters of the Andaman Islands, Bay of Bengal. Estuar. Coasts 37 (2), 381–398.

Loo, Y.Y., Billa, L., Singh, A., 2015. Effect of climate change on seasonal monsoon in Asia and its impact on the variability of monsoon rainfall in Southeast Asia. Geosci. Front. 6 (6), 817–823.

López-Medellín, X., Ezcurra, E., 2012. The productivity of mangroves in northwestern Mexico: a meta-analysis of current data. J. Coast. Conserv. 16 (3), 399–403.

Lovelock, C.E., 2008. Soil respiration and belowground carbon allocation in mangrove forests. Ecosystems 11 (2), 342–354.

Lovelock, C.E., Ruess, R.W., Feller, I.C., 2006. Fine root respiration in the mangrove Rhizophora mangle over variation in forest stature and nutrient availability. Tree Physiol. 26 (12), 1601–1606.

Lu, W., Xiao, J., Liu, F., Zhang, Y., Liu, C.A., Lin, G., 2017. Contrasting ecosystem CO_2 fluxes of inland and coastal wetlands: a meta-analysis of eddy covariance data. Glob. Chang. Biol. 23 (3), 1180–1198.
Maeght, J.L., Gonkhamdee, S., Clement, C., Isarangkool Na Ayutthaya, S., Stokes, A., Pierret, A., 2015. Seasonal patterns of fine root production and turnover in a mature rubber tree (*Hevea brasiliensis Müll.* Arg.) stand-differentiation with soil depth and implications for soil carbon stocks. Frontiers in plant science 6, 1022.
Maher, D.T., Call, M., Santos, I.R., Sanders, C.J., 2018. Beyond burial: lateral exchange is a significant atmospheric carbon sink in mangrove forests. Biol. Lett. 14 (7), 20180200.
Malhi, Y., Doughty, C., Galbraith, D., 2011. The allocation of ecosystem net primary productivity in tropical forests. Phil. Trans. R. Soc. B 366 (1582), 3225–3245.
Marchand, C., 2017. Soil carbon stocks and burial rates along a mangrove forest chronosequence (French Guiana). For. Ecol. Manag. 384, 92–99.
Muhammad-Nor, S.M., Huxham, M., Salmon, Y., Duddy, S.J., Mazars-Simon, A., Mencuccini, M., Jackson, G., 2019. Exceptionally high mangrove root production rates in the Kelantan Delta, Malaysia; an experimental and comparative study. For. Ecol. Manag. 444, 214–224.
Mukhopadhyay, S.K., Biswas, H., De, T.K., Sen, B.K., Sen, S., Jana, T.K., 2002. Impact of Sundarban mangrove biosphere on the carbon dioxide and methane mixing ratios at the NE Coast of Bay of Bengal, India. Atmos. Environ. 36 (4), 629–638. https://doi.org/10.1016/S1352-2310(01)00521-0.
Nam, V.N., Sasmito, S.D., Murdiyarso, D., Purbopuspito, J., MacKenzie, R.A., 2016. Carbon stocks in artificially and naturally regenerated mangrove ecosystems in the Mekong Delta. Wetl. Ecol. Manag. 24 (2), 231–244.
Ochoa-Gómez, J.G., Lluch-Cota, S.E., Rivera-Monroy, V.H., Lluch-Cota, D.B., Troyo-Diéguez, E., Oechel, W., Serviere-Zaragoza, E., 2019. Mangrove wetland productivity and carbon stocks in an arid zone of the Gulf of California (La Paz Bay, Mexico). For. Ecol. Manag. 442, 135–147.
Owen, L., Bhardwaj, M.S., Leinbach, T.R., 2019. Ayeyarwady River. Encyclopaedia Britannica, Inc Accessed 29th April. https://www.britannica.com/place/Ayeyarwady-River.
Phillips, C.L., Nickerson, N., 2015. Soil respiration. Reference Module in Earth Systems and Environmental Sciences.
Poffenbarger, H., Needelman, B., Megonigal, J., 2011. Salinity influence on methane emissions from tidal marshes. Official Scholarly Journal of the Society of Wetland Scientists 31 (5), 831–842. https://doi.org/10.1007/s13157-011-0197-0.
Poungparn, S., Charoenphonphakdi, T., Sangtiean, T., Patanaponpaiboon, P., 2016. Fine root production in three zones of secondary mangrove forest in eastern Thailand. Trees 30 (2), 467–474.
Pregitzer, K.S., Euskirchen, E.S., 2004. Carbon cycling and storage in world forests: biome patterns related to forest age. Glob. Chang. Biol. 10 (12), 2052–2077.
Rahman, M.M., Khan, M.N.I., Hoque, A.F., Ahmed, I., 2015. Carbon stock in the Sundarbans mangrove forest: spatial variations in vegetation types and salinity zones. Wetl. Ecol. Manag. 23 (2), 269–283.
Richards, D.R., Friess, D.A., 2016. Rates and drivers of mangrove deforestation in Southeast Asia, 2000–2012. Proc. Natl. Acad. Sci. 113 (2), 344–349.
Ritchie, H., Roser, M., 2017. CO_2 and Greenhouse Gas Emissions - Myanmar. Published online at OurWorldInData.org Retrieved August 2020 from:. https://ourworldindata.org/co2-and-other-greenhouse-gas-emissions.
Robertson, A.I., Alongi, D.M., 2016. Massive turnover rates of fine root detrital carbon in tropical Australian mangroves. Oecologia 180 (3), 841–851.
Rosentreter, J.A., Maher, D.T., Erler, D.V., Murray, R., Eyre, B.D., 2018. Seasonal and temporal CO_2 dynamics in three tropical mangrove creeks–a revision of global mangrove CO_2 emissions. Geochim. Cosmochim. Acta 222, 729–745.
Sanderman, J., Hengl, T., Fiske, G., Solvik, K., Adame, M.F., Benson, L., Duncan, C., 2018. A global map of mangrove forest soil carbon at 30 m spatial resolution. Environ. Res. Lett. 13 (5), 055002.
Sasmito, S.D., Taillardat, P., Clendenning, J.N., Cameron, C., Friess, D.A., Murdiyarso, D., Hutley, L.B., 2019. Effect of land-use and land-cover change on mangrove blue carbon: a systematic review. Glob. Chang. Biol. 25 (12), 4291–4302.
Sea, M.A., Garcias-Bonet, N., Saderne, V., Duarte, C.M., Sea, R., 2018. Carbon dioxide and methane emissions from Red Sea mangrove sediments. Biogeosciences 15, 5365–5375.
Sidik, F., Lovelock, C.E., 2013. CO_2 efflux from shrimp ponds in Indonesia. PLoS One 8 (6), e66329. https://doi.org/10.1371/journal.pone.0066329.
Sidik, F., Fernanda Adame, M., Lovelock, C.E., 2019. Carbon sequestration and fluxes of restored mangroves in abandoned aquaculture ponds. Journal of the Indian Ocean Region 15 (2), 177–192.
Sirisena, T.A.J.G., Maskey, S., Ranasinghe, R., Babel, M.S., 2018. Effects of different precipitation inputs on streamflow simulation in the Ayeyarwady River basin, Myanmar. Journal of Hydrology: Regional Studies 19, 265–278.
Spivak, A.C., Sanderman, J., Bowen, J.L., Canuel, E.A., Hopkinson, C.S., 2019. Global-change controls on soil-carbon accumulation and loss in coastal vegetated ecosystems. Nat. Geosci. 12 (9), 685–692.
Thant, Y.M., Kanzaki, M., Ohta, S., Than, M.M., 2012. Carbon sequestration by mangrove plantations and a natural regeneration stand in the Ayeyarwady Delta, Myanmar. Tropics 21 (1), 1–10.
Walcker, R., Gandois, L., Proisy, C., Corenblit, D., Mougin, E., Laplanche, C., Fromard, F., 2018. Control of "blue carbon" storage by mangrove ageing: evidence from a 66-year chronosequence in French Guiana. Glob. Chang. Biol. 24 (6), 2325–2338.
Webb, E.L., Jachowski, N.R.A., Phelps, J., Friess, D.A., Than, M.M., Ziegler, A.D., 2014. Deforestation in the Ayeyarwady Delta and the conservation implications of an internationally-engaged Myanmar. Glob. Environ. Chang. 24, 321–333.
World Weather Online, 2020. https://www.worldweatheronline.com/pyapon-weather-history/Ayeyarwady/mm.aspx.
Zöckler, C., Aung, C., 2019. The mangroves of Myanmar. Sabkha Ecosystems. Springer, Cham, pp. 253–268.